Biomedicine & Pharmacotherapy 177 (2024) 116953

Contents lists available at ScienceDirect

Biomedicine & Pharmacotherapy

journal homepage: www.elsevier.com/locate/biopha

Peroxiredoxin-2 represses NRAS-mutated melanoma cells invasion by modulating EMT markers

Isabella Harumi Yonehara Noma [a,1], Larissa Anastacio da Costa Carvalho [a,1], Denisse Esther Mallaupoma Camarena [a], Renaira Oliveira Silva [a], Manoel Oliveira de Moraes Junior [a], Sophia Tavares de Souza [a], Julia Newton-Bishop [b], Jérémie Nsengimana [c], Silvya Stuchi Maria-Engler [a,*]

[a] Department of Clinical and Toxicological Analysis, School of Pharmaceutical Sciences, University of São Paulo, Avenida Professor Lineu Prestes, 580, São Paulo, SP 05508-00, Brazil
[b] Leeds Institute of Medical Research, School of Medicine, University of Leeds, Leeds LS9 7TF, UK
[c] Biostatistics Research Group, Population Health Sciences Institute, Faculty of Medical Sciences, Newcastle University, Newcastle upon Tyne NE2 4BN, UK

ARTICLE INFO

Keywords:
Cutaneous malignant melanoma
Peroxiredoxin 2
Phenotype switching

Chemical Compounds studied in this article:
Gliotoxin (PubChem CID: 6223)

ABSTRACT

The second most common mutation in melanoma occurs in NRAS oncogene, being a more aggressive disease that has no effective approved treatment. Besides, cellular plasticity limits better outcomes of the advanced and therapy-resistant patients. Peroxiredoxins (PRDXs) control cellular processes through direct hydrogen peroxide oxidation or by redox-relaying processes. Here, we demonstrated that PRDX2 could act as a modulator of multiple EMT markers in NRAS-mutated melanomas. PRDX2 knockdown lead to phenotypic changes towards invasion in human reconstructed skin and the treatment with a PRDX mimetic (gliotoxin), decreased migration in PRDX2-deficient cells. We also confirmed the favorable clinical outcome of patients expressing PRDX2 in a large primary melanoma cohort. This study contributes to our knowledge about genes involved in phenotype switching and opens a new perspective for PRDX2 as a biomarker and target in NRAS-mutated melanomas.

1. Introduction

Melanoma of the skin is the fifth most common type of cancer [1] and the deadliest form of skin cancer due to its high metastatic potential, development of resistance and tumor recurrence [2]. The second most frequent mutation in melanoma occurs in NRAS oncogene, found in approximately 25 % of cutaneous melanoma cases, after BRAF, which affects 40–45 % of all patients [3]. NRAS-mutated melanomas are more aggressive, resulting in lower patient overall survival, and it has no specific therapy approved [4]. Immunotherapy is the first-line treatment for surgically incurable NRAS-mutated melanoma at high stages, such as anti-PD-1(nivolumab or pembrolizumab), and the combination of anti-PD-1 and CTLA-4 blockade (ipilimumab). Second-line treatment includes MEK inhibitors and combination of targeted-therapies as BRAF and MEK inhibitors. Altogether, the therapeutic success is limited for these patients by drug resistance and clinical relapse, emphasizing the need for new therapeutic approaches and new targeted combinations [3, 5].

One of the major challenges in treating metastatic melanoma is the residual disease associated with intratumoral heterogeneity and cellular plasticity. These well-characterized phenotypic switches between differentiated (proliferative) and undifferentiated (invasive) occur as cells undergo phenotypic transitions as an adaptative mechanism under stressful conditions. These phenotypes have different gene signatures, therapeutic sensitivity, and metastatic potential [6].

A common stressful condition in cancer, is when the physiological balance in the redox state is disrupted. The transient production of ROS is necessary for cell signaling, but its persistent production and exposure, can trigger tumor initiation and/or progression and also be cytotoxic. Once ROS have a dual role in cancer, agents that modulates its levels are interesting targets [7]. In this sense, cells regulate the expression of cellular peroxidase enzymes to maintain the redox homeostasis [8].

Peroxiredoxins (PRDXs) are one of the major hydrogen peroxide

* Correspondence to: Av. Professor Lineu Prestes, 580 - Bloco 17, São Paulo, SP CEP 05508-000, Brazil.
E-mail address: silvya@usp.br (S.S. Maria-Engler).
[1] These authors contributed equally to this work.

https://doi.org/10.1016/j.biopha.2024.116953
Received 12 March 2024; Received in revised form 5 June 2024; Accepted 15 June 2024
Available online 1 July 2024

Table 1
Identification of NRAS-mutated melanoma cell lines.

Cell lines	Mutation	Short-tandem-repeat
SK-MEL-147	NRAS p.Gln61Arg (c.182 A>G): Q61R (PubMed=24576830; PubMed=25728708).	Amelogenin (X); CSF1PO (10, 12); D13S317 (9, 11); D16S539 (12, 13); D5S818 (10, 13); D7S820 (9, 11); THO1 (6, 9.3); TPOX (8, 12); vWA (17, 18).
SK-MEL-173	NRAS p.Gln61Lys (c.181 C>A): Q61K (PubMed=21725359; PubMed=24576830).	Amelogenin (X, Y); CSF1PO (10, 11); D13S317 (9, 11); D16S539 (11, 12); D5S818 (9, 11); D7S820 (9, 11); THO1 (7, 9.3); TPOX (8); vWA (18).

Available: https://www.cellosaurus.org/

consumers, controlling cellular processes through direct hydrogen peroxide oxidation or by redox-relaying processes. The PRDX family is classified according to the number of active-site cysteine residues into the 1-Cys subfamily and 2-Cys (PRDX1, 2, 3, and 4), with PRDX1 and 2 being more abundant in the cytosol and nucleus [8]. Our group have previously demonstrated that PRDXs could act as biomarkers and are involved in melanoma heterogeneity and resistance [9,10]. The importance of redox regulation and the use of PRDXs as biomarkers, have also been highlighted before [11]. It has been demonstrated that PRDX2 suppresses BRAF-mutated melanoma cell proliferation and migration by increasing the E-cadherin/β-catenin complexes in adherens junctions, a critical step for metastatic ability [12]. Studies in invasive melanoma cells and metastatic tumors have already demonstrated a downregulation or silencing of PRDX2 [8,9,13,14].

Once NRAS-mutated melanomas have no effective treatment, we investigated the role of PRDX2 in this context and demonstrated that it could modulate the invasion profile, impacting the overall patient survival and also can act as a biomarker or possible target.

2. Materials and methods

2.1. Cell culture

The cell lines SK-MEL-147, SK-MEL-173 (kindly donated by Dr. María Soengas, Centro Nacional de Investigaciones Oncológicas, Madrid, Spain) were cultured in DMEM (Gibco, USA) with 10 % FBS, 25 μg/mL ampicillin, and 100 μg/mL streptomycin). Cells were cultured at 37 °C with 5 % CO_2 in a humidified chamber and passage numbers were less than 100. Cells were assayed for mycoplasma contamination every two weeks with conventional PCR. The short-tandem-repeat profiling (DNA fingerprinting) was performed using PowerPlex® 16 System (Promega) on following short-tandem-repeat loci. The results in table showed the perfect match with known profile (Table 1).

2.2. Cell viability assays

Cell viability was evaluated using the death curve assay after exposure to Gliotoxin - GT (Sigma-Aldrich /G9893–5MG) treatment. GT was solubilized in DMSO (10 mM). In a 24-well plate, 2×10^4 cells were seeded and, after adherence, they were treated with different concentrations of GT (0, 50, 100, 200 and 400 nM) for 24 hours of incubation. After staining using Trypan Blue dye (T6146, Sigma-Aldrich, St. Louis, MO, USA), viable cells were counted in a Neubauer chamber.

2.3. Growth curve

The growth curve was evaluated by counting cells in a Neubauer chamber, using the Trypan Blue dye exclusion method. Cell lines were plated at a concentration of 10^4 cells/well in triplicate. After a period of 24, 72, 120, and 168 hours the cells were collected. Then, they were incubated with Trypan Blue solution (0.4 % in PBS) for approximately 5 minutes. In this assay, non-viable cells can be identified by blue staining and counted under an optical microscope, while viable cells are not permeable to the dye [15].

2.4. Western blotting

Cell lysates for Western Blotting were prepared in RIPA buffer with a cocktail of protease inhibitors (Roche, Penzberg, Upper Bavaria, Germany) and with a cocktail of phosphatase inhibitors I and II (Santa Cruz Biotechnology, Santa Cruz, CA, USA). Total protein (40 μg) run to SDS gel electrophoresis with a 4–20 % gradient under reducing conditions and subsequent transfer to a PVDF membrane (Hybond-P, Amersham Pharmacia Biotech, Piscataway, NJ, USA). The membrane was blocked with 5 % BSA diluted in TBS-Tween 20 (50 mM Tris-HCl, pH 7.5, 150 mM NaCl, 0.1 % Tween-20) for 1 hour and the antibodies were

Table 2
shRNA sequences for PRDX2 inhibition.

Bacterial stock code	ID	Sequences	PRDX2- 201	PRDX2- 202
TRCN0000064905	PRDX2–0	CAGACGCTTGTCTGAGGATTA	Éxon 4	Éxon 4
TRCN0000064906	PRDX2–1	GTGAAGCTGTCGGACTACAAA	Éxon 2	Éxon 2
TRCN0000064907	PRDX2–2	GCCTGGCAGTGACACGATTAA	Éxon 6	Éxon 5

tested at concentrations recommended by the manufacturer (Table S1). Protein bands were detected by enhanced chemiluminescence (ECL; Amersham Pharmacia Biotech, Piscataway, NJ, USA) and semi-quantified using a Image J software.

2.5. Gene expression by real-time PCR

Total RNA from cell lines was extracted using the RNeasy Plus Mini Kit (Qiagen), according to the manufacturer's instructions. The RNA was heated to 65ºC for 5 minutes, and quantified using a spectrophotometer at 260 nm to evaluate the sample's quality. RT-PCR reaction (real-time polymerase chain reaction) was performed using the Taqman® method (Life Technologies, USA). The cDNAs obtained from the samples were diluted (2 μg/μL). Reactions had a final volume of 10 μL containing 0.5 μL of primer mix (forward and reverse) for each gene of interest (Table S2), 1 μL of cDNA, 5 μL of 2x Taqman® Gene Expression Master Mix (Life Technologies, USA), and 3.5 μL of RNAse-free water. The relative level of gene expression was calculated using the delta delta Ct method (cycle threshold method) with GAPDH as endogenous controls [16].

2.6. Clonogenic assay

The cells were seeded at 10^3 cells/well in 6-well dishes and cultured in DMEM for 2 and 3 weeks. After cell adhesion (24 hours), they were treated at different concentrations, based on the results obtained in the death curve. The culture medium was changed every 2–3 days and gliotoxin was added for a period of 15 days, varying according to the cell line used. After the colony formation period, the wells were washed with PBSA. The colonies were then fixed and stained with a solution of 49.75 % methanol, 49.75 % deionized water, and 0.5 % crystal violet. The plates were photographed to compare the treatment effects. The analysis of the number of colonies and the area they occupied was carried out according to Guzmán et al.[17].

2.7. Transwell assay

The invasion capacity of melanoma cells was evaluated after treatment of the cell lines on Transwell membranes (8 μm pore size, Becton Dickinson). These were coated with 30 μL of Matrigel (BD Biosciences, San Jose, CA, diluted 1:6 in FBS-free DMEM). Cells were resuspended (5×10^4 cells/well) in FBS-free DMEM and added to the upper compartment of the chamber. Then, 750 μL of DMEM supplemented with 10 % FBS was added to the lower chamber. Treatments were used in both upper and lower compartments. After 24 h, cells that migrated through Matrigel were fixed in 4 % formaldehyde (in 1% PBS), stained with 1 % crystal violet (in methanol) for 20 minutes before counting in an inverted microscope (Axiovert S100, Zeiss, Germany). In each well, 5 representative and independent random fields were counted (20x magnification).

2.8. Wound-healing assay

Evaluation of the ability of melanoma cells to migrate after treatment: 5×10^4cells/well were seeded in 24-well plates. After reaching approximately 90 % confluence, slits ("wounds") were made in the center of each well using a 200 μL pipette tip. The cells were then washed with 1x PBS, and treatments with DMEM culture medium + 1 % FBS were added. The experiment was carried out until the slits were closed in the controls, with pictures taken through a microscope. Analysis of cell-free areas was performed using ImageJ software.

2.9. PRDX2 gene silencing through lentiviral vectors

The silencing of the PRDX2 gene in cell lines was performed using short-hairpin RNA (shRNA) sequences to inhibit the messenger RNA (mRNA) of this gene. This process involved using bacterial cultures transfected with the Mission shRNA plasmid sequence (Sigma, USA). Three different shRNA sequences for PRDX2 were used to inhibit distinct regions of the mRNA. Bacterial stocks were cultivated for subsequent extraction and purification of plasmid DNA, following the Sigma Mission cell cloning protocol. Lentiviral vectors with a random sequence of nucleotides (scramble) were used to generate controls, which underwent the same manipulation conditions as the shRNA sequences. The shRNA vectors were co-transfected with lentiviral packaging plasmids into HEK293T cells, according to the manufacturer's instructions. These cells were selected using puromycin antibiotic (Sigma-Aldrich, USA). Afterward, the manipulated PRDX2 gene was validated by performing Western blotting and RT-PCR experiments. The knockdown cells (inhibited) were identified as scramble for the control (CN), PRDX2#0 for the cell line infected with shRNA sequence 0 PRDX2, PRDX2#1 for the cell line infected with shRNA PRDX2 sequence 1, and PRDX2#2 for the cell line infected with shRNA PRDX2 sequence 2 (Table 2).

2.10. Reconstruction of human skin (RHS) with melanoma

Primary human cells were isolated from skin samples extracted obtained from breast plastic surgery and/or postectomy in University Hospital of USP (CEP/HU-USP 943/09, SISNEP CAAE 0062.0.198.000–9). Approved was granted by Ethics Committee (CEP/FCF-USP 534). After extraction, the cells were tested for the presence of microorganisms (Human *Papillomavirus*, *Herpes Simplex* Virus, Cytomegalovirus, Hepatitis B, Hepatitis C, HIV-1, *Chlamydia trachomatis*, *Neisseria gonorrhoeae*, *Mycoplasma genitalium*, *Treponema pallidum* and *Trichomonas vaginalis*) by PCR. The reconstructed human skin model (RHS) followed the protocol described by Brohem *et al.* (2011) [18], with the following changes regarding the number of cells 50×10^4 melanoma cells/skin. The RHS were cultured and incubated submerged in DMEM:HAM F-12 1x (Gibco#21700–026) medium (1:3) + supplements (cholera toxin (1 μM), insulin (5 mg/mL), apo-transferrin (5 mg/mL), hydrocortisone-21 (0,1 mg/mL) and EGF (1 mg/mL)) for 24 hours, followed by 11 days of exposure to air-liquid interface to promote epithelial differentiation. After this period, the skins were collected, and fixed with 4 % paraformaldehyde and processed for histological analysis.

2.11. Histology and immunohistochemistry

Samples were processed according to Camarena et al., 2020 [19]. The immunostaining assay was performed using an anti-melan A antibody (ab51061) at a 1:50 dilution. A commercial kit with a goat secondary antibody against rabbit and mouse immunoglobulins (EnVision Flex/HRP, Dako Omnis, Santa Clara, CA, USA) was used in combination with 3,3′-diaminobenzidine (DAB; EnVision Flex DAB + Chromogen, Dako Omnis, Santa Clara, CA, USA) according to the manufacturer's instructions. All images were observed and photographed with an

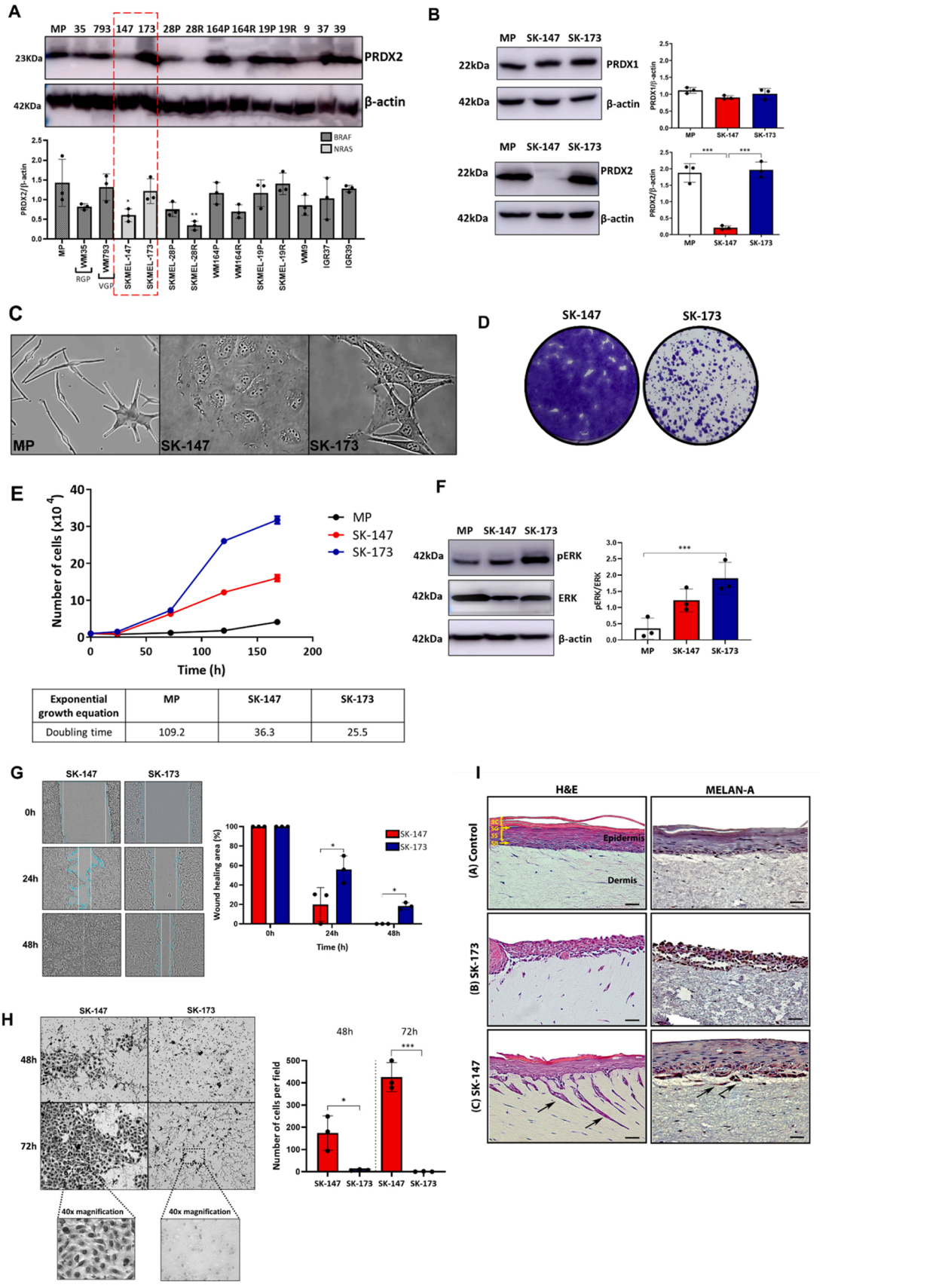

Exponential growth equation	MP	SK-147	SK-173
Doubling time	109.2	36.3	25.5

(caption on next page)

Fig. 1. PRDX2 expression in NRAS-mutated melanoma with different phenotypic profile. A Screening of the PRDX2 protein expression in different mutations and stages of melanoma cell lines (melanoma cell lines, including radial growth phase (RGP), vertical growth phase (VGP), NRAS-mutant melanoma, and BRAF-mutant melanoma). B Western blot was used to detect the protein expression of PRDX1 and PRDX2. C Cell morphology in 40x magnification. D Colony formation assay after ~15 days. E Growth curve at times 24, 72, 120 and 168 hours by trypan blue exclusion. F Western blot was used to detect the protein expression of ERK-phosphorylated. G Wound healing assay after 24 and 48 hours with wound area measurement. H Invasion assay after 48 and 72 hours and quantification of number of cells per field below of the chamber Matrigel. I Control skin without melanoma, skin with NRAS-mutant melanoma stained with Hematoxylin & Eosin and immunohistochemical staining of Melan-A, 20x magnification. Arrows indicate the sites of melanoma invasion in the dermis. Epidermis included SB: *stratum basale*, SS: *stratum spinosum*, SG: *stratum granulosum*, SC: *stratum corneum*. **A-H** All values are indicated as mean ± standard deviation (SD) of three independent experiments. P values are based on a one-way analysis of variance (ANOVA) followed by Tukey's test, *p<0.05 **p<0.01 and ***p<0.001. Images are representative of three independent biological experiments. Abbreviations: Primary melanocyte (MP), SK-MEL-147 (SK-147), and SK-MEL-173 (SK-173).

Eclipse i80 Nikon camera using the NIS-Elements Viewer (Nikon) program for image acquisition [19].

2.12. Statistical analysis

GraphPad Prism 7.0 was used for all in vitro data analysis. An independent Student's t-test was applied to two-group comparisons, while ANOVA with Tukey correction was applied to multiple groups/multiple predictors. Doubling times were obtained by non-linear regression analysis. Pairwise gene expression correlations were performed after normalizing the data, and the Pearson correlation was represented graphically. Analyses were considered significant when p-values were $\leq$ 0.05. Values were indicated as mean ± standard error of triplicate results from three independent experiments.

2.13. Patient data analysis

The Leeds melanoma cohort is a prospective cohort of patients diagnosed with primary melanoma in the North of England. These patients consented to be followed up starting from 3 to 6 months after diagnosis to monitor the risk of recurrence following the initial surgery. Death records were retrieved from the UK Office of National Statistics and confirmed by checking death certificates. Transcriptomic data were generated from primary tumor formalin-fixed paraffin-embedded (FFPE) blocks. Samples were independent and non-matched. Any duplicates included for quality control purposes were removed after data cleaning [20]. Transcriptomic data were generated using the Illumina HT12.4 DASL array. Illumina's software GenomeStudio was used to extract raw data from image files before they were exported into R Bioconductor for further processing. This processing included background correction and quantile normalization using Lumi [21], followed by batch correction by Singular Value Decomposition (SVD) in Swamp [22].

To explore the utility of in vitro results in patients, we performed the following analyses on this cohort using STATA 18 (StataCorp. 2023). Transcripts and clinical data from the Leeds Melanoma cohort are accessible in the European Genome-phenome Archive under accession number EGAS00001002922 [20]. This is one of the largest transcriptomic datasets on primary melanoma worldwide, with a sample size of 703 patients and long follow-up (>10 years).

Associations between transcripts of PRDX2 and candidate targets related to tumor progression were performed by linear regression in the entire cohort and stratified by oncogenic mutations BRAF and NRAS. Regression coefficients of these analyses were represented in a heatmap. We tested the association between PRDX2 expression and the presence/absence of BRAF and NRAS mutations using analysis of variance (ANOVA). Pearson's correlation was calculated between the expression of PRDX2 and the log-transformed Breslow thickness (the transformation allowed for an approximate normality distribution). A similar analysis was performed to test for association with tumor staging (AJCC, American Joint Committee on Cancer), and the results were plotted as violin plots or box plots.

We tested the effect of PRDX2 on melanoma-specific survival (using only deaths confirmed to be caused by melanoma) using Cox proportional hazards regression. Survival profiles were plotted with Kaplan-Meier curves. Survival analysis was performed after dividing PRDX2 expression into 5 groups (lower 20 % = 1st quintile, upper 20 % = 5th quintile). The number of 5 was arbitrarily chosen, but it is possible to merge similar groups. Finally, the top 4 quintiles (80 % of tumors with the highest PRDX2 expression) were grouped together because their effect on prognosis appeared identical.

3. Results

3.1. Investigating the role of PRDX2 in proliferation, colony formation, migration, and invasion in NRAS-mutated melanoma

Initially, we tested several cell lines with different mutations (BRAF and NRAS) and tumor stages (vertical or horizontal growth, and metastatic melanoma) to investigate the protein expression of PRDX2. Our data highlighted that, in NRAS-mutated cells, PRDX2 exhibited a distinct expression pattern (Fig. 1A). This observation led us to further investigate PRDX2 in N-RAS mutated cell as SK-MEL-147, derived from metastatic melanoma, and SK-MEL- 173, from primary melanoma.

We assessed PRDX2 protein expression and observed high levels in our control melanocyte (MP) and in SK-MEL-173 compared to SK-MEL-147. Interestingly, PRDX1 expression did not vary among the cells tested (Fig. 1B). These cells with different mutations in NRAS, exhibited different morphologies and colony formations (Fig. 1C - D). SK-MEL-173 displayed a shorter doubling time and higher phosphorylated ERK levels (Fig. 1E – F), indicating a more proliferative profile than SK-MEL-147. Conversely, SK-MEL-147 showed greater potential for migration and invasion, observed by wound healing and invasion assay (Fig. 1G - H).

Using reconstructed human skin (RHS) models, we compared the profiles of these cell lines. We observed the presence of skin layers (corneal layer of the epidermis, dermis) and the melanoma cells which were stained with Melan-A. RHS-SK-MEL-173 melanoma cells demonstrated higher proliferation, growing over the stratum corneum, whereas RHS-SK-MEL-147 melanoma cells showed more pronounced invasion, infiltrating into the dermis (Fig. 1I).

3.2. Altering the phenotypic profile of SK-MEL-173 by knocking down PRDX2

We employed shRNAs to modulate PRDX2 expression and conducted knockdown (KD) experiments. The specificity of the shRNA was validated through Western Blot analysis, which showed a reduction specifically in the PRDX2 isoform. With shRNA PRDX2 sequence 1 (shPRDX2#1), we observed partial inhibition, and with shRNA PRDX2 sequence 2 (shPRDX2#2), there was more than a 60 % inhibition compared to the control – scramble (shSCR). We discarded shPRDX2#0 due to its lack of inhibitory effect (Fig. 2A - B).

Throughout our study, no differences were noted in the cell lines' morphology or colony formation characteristics (Fig. 2C - D). Post-KD experiments, the cells maintained their doubling time and phosphorylated ERK levels without statistically significant changes (Fig. 2E – F). The cells with shPRDX2#2 demonstrated more invasiveness capacity in transwell assay and in the reconstructed human skin model. However, we did not observe significative changes in the migration assay (Fig. 2G – H).

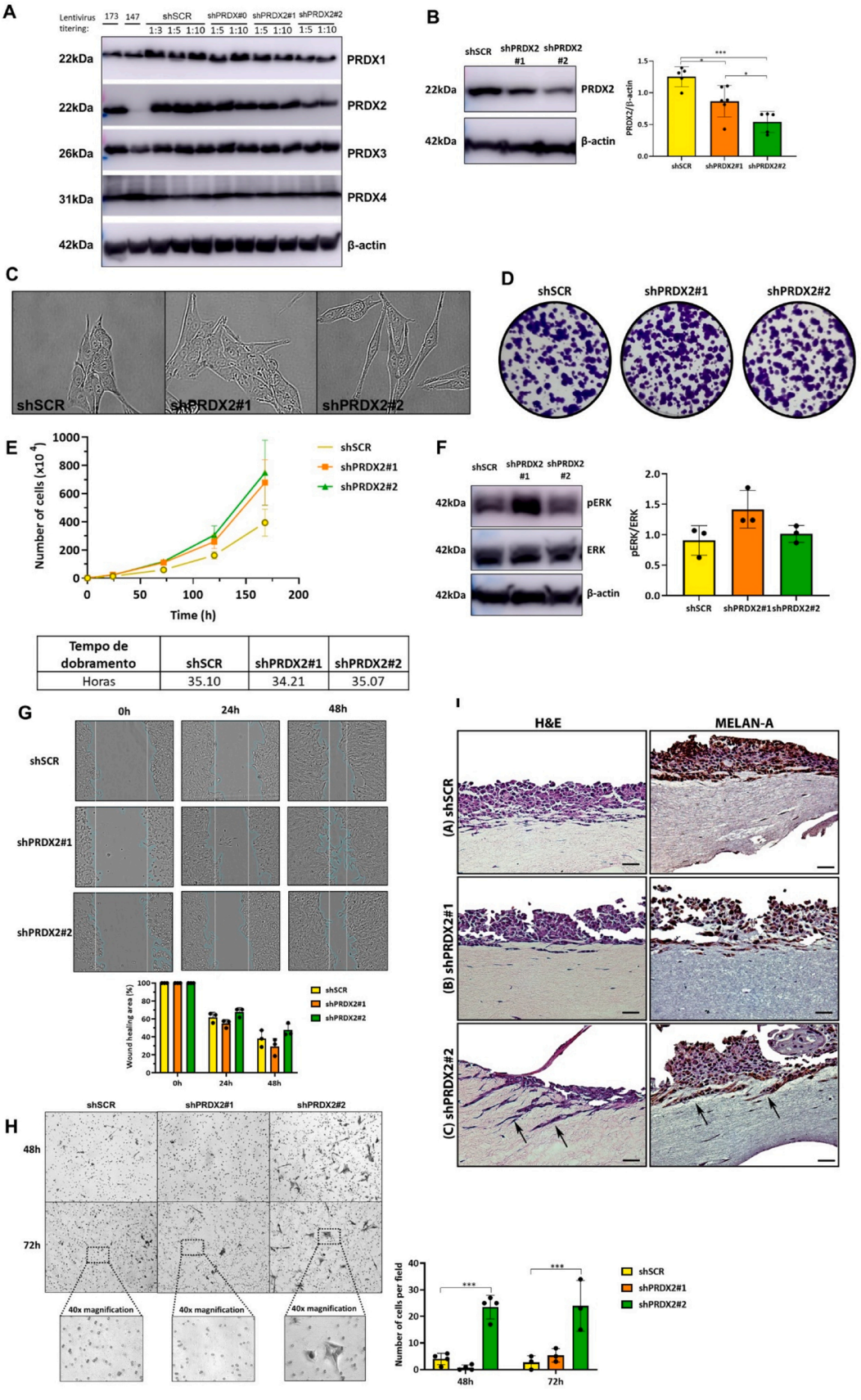

Tempo de dobramento	shSCR	shPRDX2#1	shPRDX2#2
Horas	35.10	34.21	35.07

(caption on next page)

Fig. 2. Knockdown (KD) of PRDX2 by shRNA changed phenotypic profile in melanoma SK-MEL-173. A Western blotting analysis of 2-cys PRDX group proteins (PRDX1, PRDX2, PRDX3 and PRDX4). B Western blot was used to detect the protein expression of PRDX2 in cells KD PRDX2. C Cell morphology in 40x magnification. D Colony formation assay after ~15 days. E Growth curve at times 24, 72, 120 and 168 hours by trypan blue exclusion. F Western blot was used to detect the protein expression of ERK-phosphorylated. G Wound healing assay after 24 and 48 hours with wound area measurement. H Invasion assay after 48 and 72 hours and quantification of number of cells per field below of the chamber Matrigel. I Control skin without melanoma, skin with melanoma KD PRDX2 (shPRDX2#1 and shPRDX2#2 compared to shSCR- scramble) stained with Hematoxylin & Eosin and immunohistochemical staining of Melan-A, 20x magnification. Arrows indicate the sites of melanoma invasion in the dermis. A-H All values are indicated as mean ± standard deviation (SD) of three independent experiments. P values are based on a one-way analysis of variance (ANOVA) followed by Tukey's test, *$p<0.05$ **$p<0.01$ and ***$p<0.001$. Images are representative of three independent biological experiments.

In the RHS model, the control (shSCR) exhibited the same pattern as naive SK-MEL-173 (Fig. 1I). KD with shPRDX2#1 showed no difference, but KD with shPRDX2#2 revealed a notable increase in skin invasion (Fig. 2I). The skins were also subjected to immunohistochemistry (IHC) staining for Melan-A to confirm the invasion of melanoma cells. These results corroborate the observed differences in invasion in the 2D model following PRDX2 knockdown.

3.3. Expression of PRDX2 alters several genes and proteins related to invasion markers: a comparison between melanoma cell lines SK-MEL-147 and SK-MEL-173

Following the observation of phenotypic changes associated with PRDX2 downregulation, we investigated the potential proteins and genes that might be influenced by PRDX2. Our data revealed a higher expression of MITF in SK-MEL-173 (where PRDX2 levels are higher), contrasting with the expression of AXL (Fig. 3A-B). However, there was no significant difference in the expression of SOX10 (Fig. 3C). Only SK-MEL-147 (where PRDX2 levels are lower) showed expression of N-cadherin (Fig. 3D). β-catenin exhibited a pattern similar to MITF, being more highly expressed in SK-MEL-173 (Fig. 3E). E-cadherin was exclusively expressed in melanocytes (MP) and not in the melanoma cells (Fig. 3F). Additionally, real-time PCR analysis of gene expression confirmed higher expression of PRDX2 and MITF, and lower expression of AXL, FN1, SNAI1, and SMAD3 in SK-MEL-173 compared to SK-MEL-147 (Fig. 3G).

3.4. Comparing PRDX2 knockdown in melanoma SK-MEL-173: control (shSCR) vs. shPRDX2#1 and shPRDX2#2

We observed that PRDX2 KD decreased the expression of MITF compared to control (scramble). The PRDX2 KD did not affect SOX10 expression, but it increased Snail expression at the protein level (Fig. 3H-K). In SK-MEL-173, AXL, N-cadherin, and E-cadherin were not expressed; therefor, the knockdown of PRDX2 in Sk-MEL-173 did not impact its expression (data not shown). Real-time PCR analysis for gene expression revealed that PRDX2 KD led to decreased levels of PRDX2, MITF, and SMAD2, and an increase in AXL and SNAI1 (Fig. 3L).

3.5. Gliotoxin (GT) treatment in NRAS-mutated melanoma

We evaluated gliotoxin (GT) as PRDX mimetic with antioxidant properties. Our viability tests revealed that melanoma cells were more sensitive to GT compared to fibroblast (FB) cells. However, there was no significant difference in sensitivity between melanocytes and the tested melanoma cell lines (Fig. 4A). The ability to form colonies was significantly reduced across all cell lines (Fig. 4B). Additionally, SK-MEL-173 cells showed no change in migration after GT treatment, whereas SK-MEL-147 cells exhibited a decrease in migration following GT treatment (Fig. 4C-D). Although GT did not affect cell proliferation, it altered the migration capability in SK-MEL-147 cells, which have lower PRDX2 levels.

3.6. Patient analysis in the Leeds Melanoma Cohort (LMC) of primary melanoma tumors

3.6.1. Gene correlation with PRDX2 in the total cohort and specifically in tumors exhibiting NRAS mutations

We validated our *in vitro* findings through bioinformatic analysis of patient data from the Leeds Melanoma Cohort (LMC, ethical approval MREC 1/3/57, PIAG 3–09(d)/2003). This analysis showed a positive correlation of PRDX2 with STAT3, CTNNB1, and CDH1, consistent with our *in vitro* assays, and a negative correlation with ZEB2, MAPK1, HIF1A, and PDGFB, which are genes implicated in tumor progression (Fig. 5A, all correlation coefficients are highly significant with $P<0.0001$). The cohort was subdivided into subgroups based on mutation type (BRAF, NRAS, and double wild type WT). It was observed that melanomas with NRAS mutations exhibited lower PRDX2 expression compared to those with BRAF mutations (Fig. 5B, $p=10^{-5}$). Despite that, PRDX2 did not have a difference in patient survival from the NRAS melanoma cohort (Sup. Fig. 1), suggesting PRDX2 is melanoma mutation-independent. Within the NRAS-mutated melanomas, PRDX2 showed varying correlations with different genes. It was negatively correlated with CSNK1A1, NRAS, AXL, and FN1, and positively correlated with ROS1, KRT18, AXIN1, and others, corroborating some of our *in vitro* results (Fig. 5C).

*3.6.2. **PRDX2 as a positive prognostic factor in the Leeds Melanoma Cohort (LMC)***

Primary melanomas from LMC patients were analyzed to corroborate our *in vitro* data. The results indicated that patients in the top 4 quintiles for PRDX2 expression (80 % high expressors) had a better survival profile compared to those with lower tumor PRDX2 expression (i.e. low expression has a double of hazard of high expression) (Fig. 5D-E). Consistent with this, lower expression of PRDX2 was associated with a more advanced stage of melanoma as indicated by AJCC stage (Fig. 5F) (mean values are 7.84 for AJCC stage I, 7.57 for AJCC stage 2 and 3) or Breslow thickness (Fig. 5G). Put together, our findings in *in vitro* and clinical datasets (especially in a large unbiased population-based cohort) suggest that PRDX2 expression in tumors is a favorable prognostic factor in primary melanomas, regardless of mutation status.

4. Discussion

PRDX2 is an antioxidant enzyme that plays an important role in redox homeostasis during carcinogenesis and in several cellular processes. While some studies have investigated the role of PRDX2 in melanomas, they were limited to BRAF-mutated melanomas, and the mechanism by which this protein contributes to melanoma progression has not been completely explored. Therefore, our aim was to understand the role of PRDX2 in NRAS-mutated melanoma and how it may influence cellular phenotypic pathways.

Our results showed that cell lines with higher PRDX2 expression have a more proliferative profile, whereas those with lower PRDX2 expression exhibit a more invasive profile. This aligns with other studies that linked PRDX2 silencing to increased migration and invasion in BRAF-mutated melanomas and gastric tumors [12,23]. Several studies have noted that MITF expression promotes proliferation and suppresses invasiveness [6,24]. Additionally, β-catenin, involved in adherens

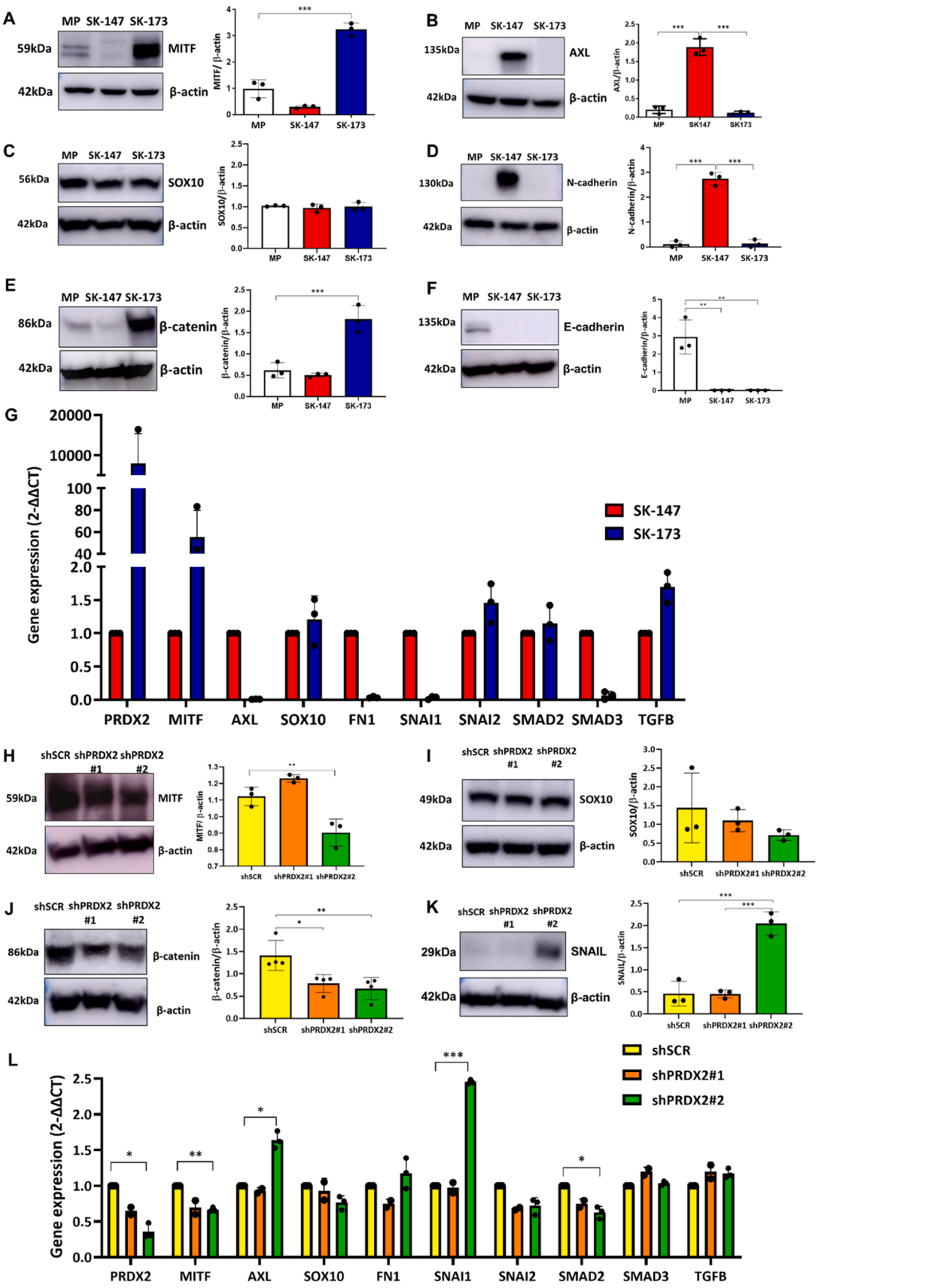

(caption on next page)

Fig. 3. Lack of PRDX2 expression promotes invasive properties by regulation of genes and proteins related MITF and EMT markers in NRAS-mutated melanoma. A Western blot was used to detect the protein expression of MITF, (B) AXL, (C) SOX10, (D) N-cadherin, (E) β-catenin and (F) E-cadherin in NRAS-mutant melanoma cell lines (SK-MEL-147 and SK-MEL-173). G Genes expressions in NRAS-mutant melanoma cell lines based in delta delta CT. H Western blot was used to detect the protein expression of MITF, (I) SOX10, (J) β-catenin and (K) Snail in melanoma KD PRDX2. L Genes expressions in melanoma KD PRDX2 based in delta delta CT. **A-L** All values are indicated as mean ± standard deviation (SD) of three independent experiments. P values are based on a one-way analysis of variance (ANOVA) followed by Tukey's test, *p<0.05 **p<0.01 and ***p<0.001. Images are representative of three independent biological experiments. Abbreviations: Primary melanocyte (MP), SK-MEL-147 (SK-147), SK-MEL-173 (SK-173), PRDX2 knockdown using shRNA: scramble sequence (shSCR), sequence 1 (shPRDX2#1), and sequence 2 (shPRDX2#2).

junctions complexes [12], cooperates with the canonical Wnt pathway [25]. This pathway is important for MAP kinase signaling, regulating MITF expression and activity, and promoting melanoma proliferation [25]. Our data demonstrated that silencing PRDX2 correlates with decreased β-catenin and MITF levels, leading to increased cell migration and invasion.

Alterations in MITF expression levels are linked to phenotypic plasticity, and the acquisition of migration and invasion capabilities. Extremely low MITF expression is characteristic of invasive melanoma cells, while high MITF expression characterizes non-invasive melanoma cells. Phenotypic plasticity refers to the ability of malignant melanoma cells to undergo transient and reversible morphological and functional changes, similar to the embryonic neural crest invasion program. Although this phenotype switching resembles epithelial-mesenchymal transition (EMT), this term is not entirely appropriate for melanoma, as melanocytes are not epithelial cells. Instead, EMT-like processes, which play a key role during the formation and migration of neural crest cells, are considered [26,27]. Epithelial-mesenchymal transition-regulating transcription factors can induce EMT-like phenotype switching in melanoma, involving proteins like SNAIL, TWIST, and ZEB [28]. Melanocyte proliferation and differentiation from neural crest precursors heavily depend on the canonical WNT signaling pathway, mediated through β-catenin, which regulates MITF [26].

In the non-canonical pathway, blocking β-catenin expression and increasing Snail expression leads to metastasis. Snail (encoded by the SNAI1 gene) and Slug (encoded by the SNAI2 gene) are transcriptional repressors. Snail is expressed in mesenchymal cells and is upregulated during EMT, while Slug is expressed in epithelial cells. This is in line with our findings, where PRDX2 knockdown increased Snail expression and invasion. This coincides with an increase in N-cadherin, a major component of the cytoskeleton in mesenchymal cells and a marker of EMT [29,30]. FN1, the gene encoding fibronectin, shows a negative correlation with PRDX2 expression. Fibronectin is an extracellular matrix component facilitating tumor progression, expressed in the metastatic niches of lung melanoma cells and identified as a regulator of the Wnt/β-catenin pathway [31]. SMAD4 mediates canonical TGF-β signaling, essential for melanoma cell proliferation *in vivo*. A TGF-β family member, BMP7, stimulates melanoma cell proliferation [26].

We validated our 2D results in three-dimensional reconstructed human skin (RHS) models. This model replicates human skin histology and is used for functional analysis of melanoma development. The radial growth phase of melanoma, occurs proliferation of cancer cells in the dermal reconstruct, and the vertical growth phase, the cells invaded deep into the dermis, similar to *in vivo* scenarios [18,32]. The RHS using SK-MEL-173, the cell line containing higher levels of PRDX2, exhibited higher rates of cell proliferation, leading to an increased proportion of melanoma in the skin, surpassing the epidermis. Conversely, the SK-MEL-147 cell line, that showed lower levels of PRDX2, displayed invasion sites in the dermis due to its high invasive capacity observed in transwell assays (2D model). In the RHS using the melanoma cell line SK-MEL-173 KD for PRDX2 (shPRDX2#2), the reduction of PRDX2 in the more proliferative cell line, resulted in an increased invasion sites, evidencing the phenotypic modulatory potential of PRDX2. Our data suggest a metastatic potential in NRAS-mutated melanoma with lower PRDX2 expression, which is consistent with several studies that demonstrated the negative regulation of PRDX2 gene in metastatic melanomas [9,12,33].

Gliotoxin, an antioxidant compound described as a 2-Cys-PRDX mimetic, can reduces H_2O_2 and be restored by accepting electrons from NADPH via the TR-Trx redox system [34]. Viability assays conducted post-GT treatment revealed no differences between lineages. However, continuous GT exposure for over three weeks decreased colony formation in all tested cell lines. Notably, only the SK-MEL-147 cell line, lacking PRDX2, exhibited a difference in migration in response to GT treatment. This suggests that GT may have a compensatory effect in the absence of PRDX in SK-MEL-147 cells, changing their profile after mimetic use. This observation aligns with another study which observed a reduction in migration using GT in BRAF-melanoma [12].

In the analysis of patient samples, several genes exhibited distinct correlations with PRDX2, with notable differences observed in ZEB2 and STAT3. ZEB2 (Zinc finger E-box binding homeobox 2) negatively correlated with PRDX2 and is known to be associated with the E-cadherin promoter, thus activating the EMT pathway and contributing to metastatic invasions [35,36]. PRDX2 also regulates STAT3-mediated transcriptional activity through redox mechanisms, transferring oxidative equivalents to STAT3, hence their positive correlation [37].

Interestingly, melanomas with NRAS mutations had lower PRDX2 expression than those with BRAF mutations. Which may explain in part the more aggressive NRAS-mutated melanoma profile. When analyzed by mutation type, the NRAS group showed different gene correlations. Within the NRAS-mutant melanoma cohort, there were increases in ROS1 and KRT18 expression, and a decrease in CSNK1A1, all correlated with PRDX2. ROS1, a receptor tyrosine kinase involved in various cancers, regulates cell proliferation, differentiation, and growth [38]. KRT18 contributes to cytoskeletal filaments that influence cell architecture [39]. Additionally, CSNK1A1 plays a role in cytoskeletal dynamics and cell motility, with its increased expression associated with metastasis [40]. An inverse relationship between PRDX2 and EMT gene signatures was observed.

We analyzed primary tumors from the Leeds' cohort *in silico*. PRDX2 had a significant impact on survival across the entire cohort of primary tumor patients (n=703, 204 deaths); very low expression of PRDX2 was detrimental (only deaths from melanoma were analyzed). Additionally, these data revealed that tumors with lower PRDX2 expression exhibited higher Breslow thickness and staging, indicating higher malignancy levels [41,42]. These clinical findings suggest the potential of PRDX2 as a biomarker in metastatic melanoma. In an osteosarcoma study, PRDX2 has already been used as a biomarker to predict treatment response [43].

Although we have not conducted *in vivo* analyses, our data aligns with findings already observed in studies using mouse models with BRAF melanoma. Furthermore, we established an *in silico* relationship using patient data, which is highly relevant for prospecting this target in a clinical context. Nevertheless, our PRDX2 baseline results with high and low PRDX2 expression strongly indicate these relationships. Despite these limitations, this study has contributed to understanding the role of PRDX2 as a target and biomarker for metastatic melanoma, particularly in NRAS-mutated.

In conclusion, our data demonstrated that PRDX2 modulates EMT-like proteins such as MITF, β-catenin, N-cadherin, and Snail, which participate in the migration/invasion process. Also, PRDX2 is associated with favorable clinical features, and Gliotoxin could be used as a potential treatment. Furthermore, we established an *in silico* relationship using patient data, which is highly relevant for prospecting this target in a clinical context. This study contributes to our knowledge about genes

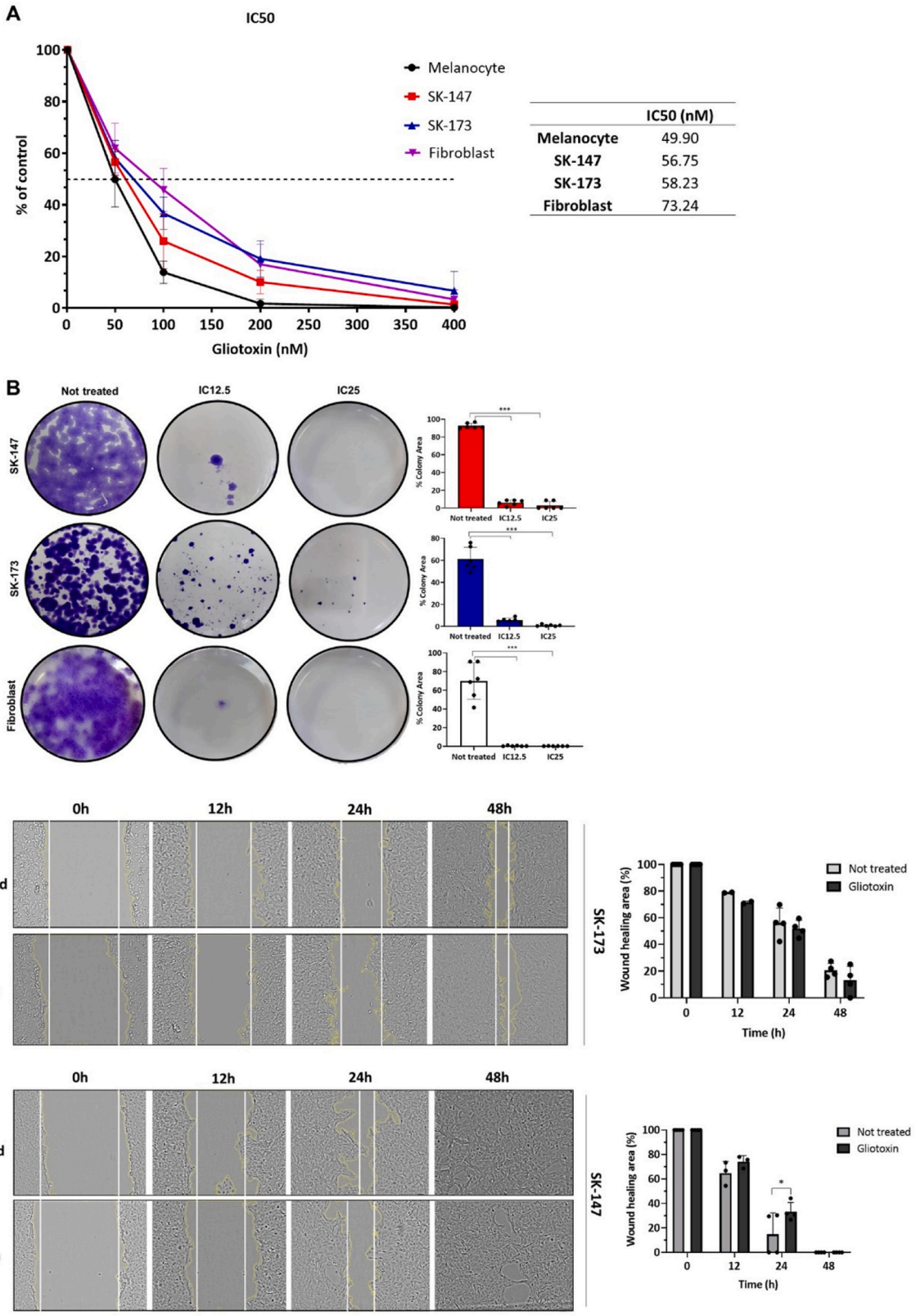

Fig. 4. Mimetic of PRDX2 inhibits cell proliferation, colony formation and migration ability in NRAS-melanoma cells. A Viability curve and table with calculated IC50 values. B Glyotoxin sensitivity test on NRAS-mutated melanoma and fibroblast (FP) cell lines for colony formation compared to untreated control using IC25 and IC12.5 concentration. Statistical analysis was performed by one-way analysis of variance (ANOVA) followed by Tukey's test, ***p<0.001, **p<0.01 and *p<0.05. C-D Wound healing test for SK-MEL-173 and SK-MEL-147 with IC75 (99.7 nM for SK-MEL-147 and 114.1 nM for SK-MEL-173). Statistical analysis was performed by two-way analysis of variance (ANOVA) followed by Tukey's test, ***p<0.001, **p<0.01 and *p<0.05. A-D Values are indicated as mean ± SD of triplicate results from three independent experiments. Abbreviations: Primary melanocyte (MP), SK-MEL-147 (SK-147), and SK-MEL-173 (SK-173).

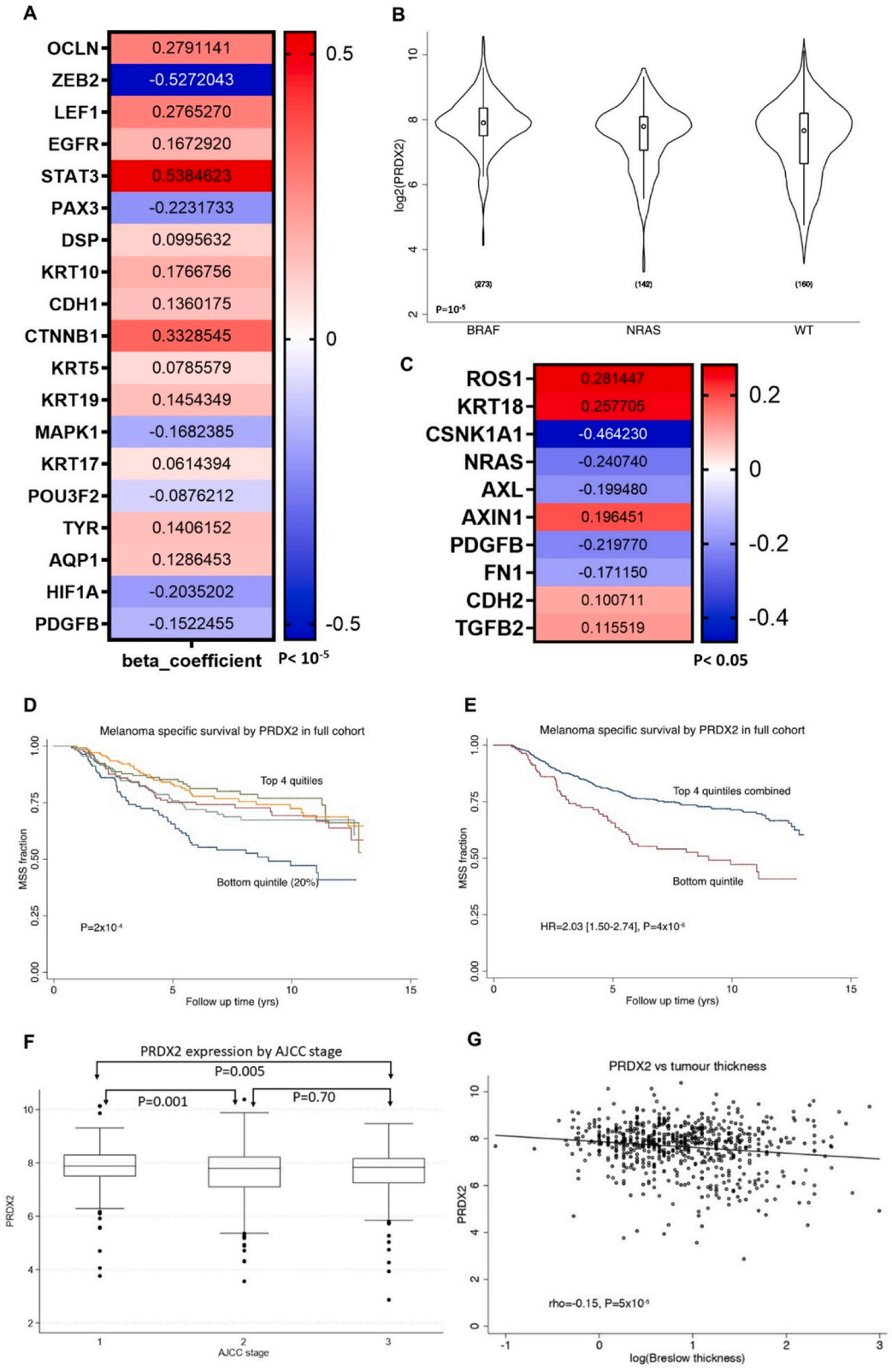

Fig. 5. Bioinformatic analysis in LMC from melanoma primary tumors: PRDX2 correlation with other genes and clinic features. A and C Regression coefficients between the expression of PRDX2 and other genes in primary melanomas in the whole LMC (n=703). Negative coefficients indicate a negative correlation while positive coefficients indicate a positive correlation. B PRDX2 tumor expression by mutation status (WT=double wild type, Pvalue=10^{-5}). C Regression coefficients between expressions of PRDX2 and other genes in NRAS-mutated primary melanoma subset of LMC (all Pvalues<0.001). D-E Melanoma specific survival (MSS) by PRDX2 in full cohort: the first 4 quintiles (80 % with high PRDX2 expression) were grouped after they appeared to have identical prognosis profiles. F Correlation of PRDX2 expression with primary tumor staging (AJCC). G Correlation of PRDX2 expression with the Breslow thickness of primary melanomas.

involved in phenotype switching and opens a new perspective for PRDX2 as a biomarker and target in NRAS-mutated melanomas.

Funding

The Leeds Melanoma Cohort was recruited using grants CRUK C588/A19167, C8216/A6129, C588/A10721 and NIH CA83115. FAPESP (#17/04926–6, #18/14936-1, #20/14019-9, #20/15042-4, 22/08041-7, #22/09245-5) and CNPq (#408769/2018, #304339/2017–2, #142058/2020-3, #309440/2021-1). This study was financed in part by the Coordenação de Aperfeiçoamento de Pessoal de Nível Superior – Brazil (CAPES) – Finance Code 001.

CRediT authorship contribution statement

Jérémie Nsengimana: Formal analysis, Data curation. **Julia-Newton Bishop:** Formal analysis, Data curation. **Sophia Tavares de Souza:** Methodology. **Manoel Oliveira de Moraes Junior:** Methodology, Formal analysis. **Renaira Oliveira Silva:** Methodology, Formal analysis. **Denisse Esther Mallaupoma Camarena:** Methodology, Formal analysis. **Larissa Anastacio da Costa Carvalho:** Writing – review & editing, Methodology, Data curation, Conceptualization, Formal analysis. **Isabella Harumi Yonehara Noma:** Writing – original draft, Methodology, Formal analysis, Data curation, Conceptualization. **Silvya Stuchi Maria-Engler:** Writing – review & editing, Supervision, Project administration, Funding acquisition, Conceptualization.

Declaration of Competing Interest

The authors declare that they have no known competing financial interests or personal relationships that could have appeared to influence the work reported in this paper.

Data availability

Data will be made available on request.

Acknowledgements

The authors are grateful for the institutional support of the School of Pharmaceutical Sciences and Central Multiusuario de Imagens Pre-Clinicas FCF-IPEN- MicroPET, University of São Paulo. Also thankful to Silvia Romano de Assis, Walter Miguel Turato, Julia Rezende da Silva, Érica Aparecida de Oliveira, Larissa Sekimoto, and all collaborators.

Appendix A. Supporting information

Supplementary data associated with this article can be found in the online version at doi:10.1016/j.biopha.2024.116953.

References

[1] R.L. Siegel Mph, K.D. Miller, N. Sandeep, W. Mbbs, | Ahmedin, J. Dvm, R.L. Siegel, Cancer statistics, 2023, CA, Cancer J. Clin. 73 (2023) 17–48, https://doi.org/10.3322/CAAC.21763.

[2] F. Huang, F. Santinon, R.E. Flores González, S.V. del Rincón, Melanoma Plasticity: Promoter of Metastasis and Resistance to Therapy, Front. Oncol. 11 (2021), https://doi.org/10.3389/FONC.2021.756001.

[3] T. Randic, I. Kozar, C. Margue, J. Utikal, S. Kreis, NRAS mutant melanoma: Towards better therapies, Cancer Treat. Rev. 99 (2021), https://doi.org/10.1016/J.CTRV.2021.102238.

[4] D.B. Johnson, I. Puzanov, Treatment of NRAS-mutant melanoma, Curr. Treat. Options Oncol. 16 (2015) 15, https://doi.org/10.1007/s11864-015-0330-z.

[5] M. Berger, G. Richtig, K. Kashofer, A. Aigelsreiter, E. Richtig, The window of opportunities for targeted therapy in BRAFwt/NRASwt/KITwt melanoma: biology and clinical implications of fusion proteins and other mutations, G. Ital. Di Dermatol. e Venereol. Organo Uff. Soc. Ital. Di Dermatol. e Sifilogr. 153 (2018) 349–360, https://doi.org/10.23736/S0392-0488.18.05970-9.

[6] F. Rambow, J.C. Marine, C.R. Goding, Melanoma plasticity and phenotypic diversity: therapeutic barriers and opportunities, Genes Dev. 33 (2019) 1295–1318, https://doi.org/10.1101/GAD.329771.119.

[7] J. Wang, D. Sun, L. Huang, S. Wang, Y. Jin, Targeting Reactive Oxygen Species Capacity of Tumor Cells with Repurposed Drug as an Anticancer Therapy, Oxid. Med. Cell. Longev. 2021 (2021), https://doi.org/10.1155/2021/8532940.

[8] S.W. Kang, S. Lee, J.H.S. Lee, Cancer-Associated Function of 2-Cys Peroxiredoxin Subtypes as a Survival Gatekeeper, Antioxid. (Basel, Switz.) 7 (2018), https://doi.org/10.3390/ANTIOX7110161.

[9] L.A.C. Carvalho, R.G. Queijo, A.L.B. Baccaro, Á.D.D. Siena, W.A. Silva, T. Rodrigues, S.S. Maria-Engler, Redox-Related Proteins in Melanoma Progression, Antioxid. (Basel, Switz.) 11 (2022), https://doi.org/10.3390/ANTIOX11030438.

[10] L.A.C. Carvalho, I.H.Y. Noma, A.H. Uehara, Á.D.D. Siena, L.H. Osaki, M.P. Mori, N. C. Souza-Pinto, V.M. Freitas, W.A.S. Junior, K.S.M. Smalley, S.S. Maria-Engler, Modeling Melanoma Heterogeneity In Vitro: Redox, Resistance and Pigmentation Profiles, Antioxid. (Basel, Switz.) 13 (2024), https://doi.org/10.3390/antiox13050555.

[11] H.R. Hintsala, Y. Soini, K.M. Haapasaari, P. Karihtala, Dysregulation of redox-state-regulating enzymes in melanocytic skin tumours and the surrounding microenvironment, Histopathology 67 (3) (2015) 348–357, https://doi.org/10.1111/his.12659. PMID: 25627040.

[12] D.J. Lee, D.H. Kang, M. Choi, Y.J. Choi, J.Y. Lee, J.H. Park, Y.J. Park, K.W. Lee, S. W. Kang, Peroxiredoxin-2 represses melanoma metastasis by increasing E-cadherin/β-catenin complexes in adherens junctions, Cancer Res 73 (2013) 4744–4757, https://doi.org/10.1158/0008-5472.CAN-12-4226/650915/AM/PEROXIREDOXIN-2-REPRESSES-MELANOMA-METASTASIS-BY.

[13] S.W. Kang, S.G. Rhee, T.S. Chang, W. Jeong, M.H. Choi, 2-Cys peroxiredoxin function in intracellular signal transduction: therapeutic implications, Trends Mol. Med. 11 (2005) 571, https://doi.org/10.1016/J.MOLMED.2005.10.006.

[14] N. Chandimali, D.K. Jeong, T. Kwon, Peroxiredoxin II Regulates Cancer Stem Cells and Stemness-Associated Properties of Cancers, Cancers (Basel) 10 (2018), https://doi.org/10.3390/CANCERS10090305.

[15] F. Liu, Y. Fu, F.L. Meyskens, MiTF regulates cellular response to reactive oxygen species through transcriptional regulation of APE-1/Ref-1, J. Invest. Dermatol. 129 (2009) 422–431, https://doi.org/10.1038/JID.2008.255.

[16] K.J. Livak, T.D. Schmittgen, Analysis of relative gene expression data using real-time quantitative PCR and the 2(-Delta Delta C(T)) Method, Methods 25 (2001) 402–408, https://doi.org/10.1006/METH.2001.1262.

[17] C. Guzmán, M. Bagga, A. Kaur, J. Westermarck, D. Abankwa, ColonyArea: an ImageJ plugin to automatically quantify colony formation in clonogenic assays, PLoS One 9 (2014) e92444, https://doi.org/10.1371/journal.pone.0092444.

[18] C.A. Brohem, L.B. Da Silva Cardeal, M. Tiago, M.S. Soengas, S.B. De Moraes Barros, S.S. Maria-Engler, Artificial skin in perspective: concepts and applications, Pigment Cell Melanoma Res 24 (2011) 35–50, https://doi.org/10.1111/J.1755-148X.2010.00786.X.

[19] D.E.M. Camarena, L.S.A.S. Matsuyama, S.S. Maria-Engler, L.H. Catalani, Development of Epidermal Equivalent from Electrospun Synthetic Polymers for In Vitro Irritation/Corrosion Testing, Nanomater. 2020, Vol. 10, Page 2528 10 (2020) 2528, https://doi.org/10.3390/NANO10122528.

[20] J. Nsengimana, J. Laye, A. Filia, S. O'Shea, S. Muralidhar, J. Poźniak, A. Droop, M. Chan, C. Walker, L. Parkinson, J. Gascoyne, T. Mell, M. Polso, R. Jewell, J. Randerson-Moor, G.P. Cook, D.Timothy Bishop, J. Newton-Bishop, β-Catenin-mediated immune evasion pathway frequently operates in primary cutaneous melanomas, J. Clin. Invest. 128 (2018) 2048–2063, https://doi.org/10.1172/JCI95351.

[21] P. Du, W.A. Kibbe, S.M. Lin, lumi: a pipeline for processing Illumina microarray, Bioinformatics 24 (2008) 1547–1548, https://doi.org/10.1093/BIOINFORMATICS/BTN224.

[22] M. Lauss, I. Visne, A. Kriegner, M. Ringnér, G. Jönsson, M. Höglund, Monitoring of technical variation in quantitative high-throughput datasets, Cancer Inf. 12 (2013) 193–201, https://doi.org/10.4137/CIN.S12862.

[23] S.H. Hong, C. Min, Y. Jun, D.J. Lee, S.H. Kim, J.H. Park, J.H. Cheong, Y.J. Park, S. Y. Kim, S. Lee, S.W. Kang, Silencing of peroxiredoxin II by promoter methylation is necessary for the survival and migration of gastric cancer cells, Exp. Mol. Med. 50 (2018), https://doi.org/10.1038/EMM.2017.267.

[24] J. Müller, O. Krijgsman, J. Tsoi, L. Robert, W. Hugo, C. Song, X. Kong, P.A. Possik, P.D.M. Cornelissen-Steijger, M.H.G. Foppen, K. Kemper, C.R. Goding, U. McDermott, C. Blank, J. Haanen, T.G. Graeber, A. Ribas, R.S. Lo, D.S. Peeper, Low MITF/AXL ratio predicts early resistance to multiple targeted drugs in melanoma, Nat. Commun. 5 (2014), https://doi.org/10.1038/NCOMMS6712.

[25] M.R. Webster, C.H. Kugel, A.T. Weeraratna, The Wnts of change: How Wnts regulate phenotype switching in melanoma, Biochim. Biophys. Acta 1856 (2015) 244–251, https://doi.org/10.1016/J.BBCAN.2015.10.002.

[26] S.M. Hossain, M.R. Eccles, Phenotype Switching and the Melanoma Microenvironment; Impact on Immunotherapy and Drug Resistance, Int. J. Mol. Sci. 24 (2023), https://doi.org/10.3390/ijms24021601.

[27] E. Tuncer, R.R. Calçada, D. Zingg, S. Varum, P. Cheng, S.N. Freiberger, C.-X. Deng, I. Kleiter, M.P. Levesque, R. Dummer, L. Sommer, SMAD signaling promotes melanoma metastasis independently of phenotype switching, J. Clin. Invest. 129 (2019) 2702–2716, https://doi.org/10.1172/JCI94295.

[28] B.De Craene, G. Berx, Regulatory networks defining EMT during cancer initiation and progression, Nat. Rev. Cancer 13 (2013) 97–110, https://doi.org/10.1038/nrc3447.

[29] L. Hao, J.R. Ha, P. Kuzel, E. Garcia, S. Persad, Cadherin switch from E- to N-cadherin in melanoma progression is regulated by the PI3K/PTEN pathway

through Twist and Snail, Br. J. Dermatol. 166 (2012) 1184–1197, https://doi.org/10.1111/J.1365-2133.2012.10824.X.
[30] D. Ribatti, R. Tamma, T. Annese, Epithelial-Mesenchymal Transition in Cancer: A Historical Overview, Transl. Oncol. 13 (2020), https://doi.org/10.1016/J.TRANON.2020.100773.
[31] S. Spada, A. Tocci, F. Di Modugno, P. Nisticò, Fibronectin as a multiregulatory molecule crucial in tumor matrisome: from structural and functional features to clinical practice in oncology, J. Exp. Clin. Cancer Res. 40 (2021), https://doi.org/10.1186/S13046-021-01908-8.
[32] A. Leikeim, M. Wußmann, F.F. Schmidt, N.G.B. Neto, F. Benz, K. Tiltmann, C. Junger, M.G. Monaghan, B. Schilling, F.K. Groeber-Becker, A preclinical model of cutaneous melanoma based on reconstructed human epidermis, Sci. Rep. 12 (2022), https://doi.org/10.1038/S41598-022-19307-0.
[33] F. Carta, P.R. Demuro, C. Zanini, A. Santona, D. Castiglia, S. D'Atri, P.A. Ascierto, M. Napolitano, A. Cossu, B. Tadolini, F. Turrini, A. Manca, M.C. Sini, G. Palmieri, C. Rozzo, Analysis of candidate genes through a proteomics-based approach in primary cell lines from malignant melanomas and their metastases, Melanoma Res 15 (2005) 235–244, https://doi.org/10.1097/00008390-200508000-00002.
[34] H.S. Choi, J.S. Shim, J.A. Kim, S.W. Kang, H.J. Kwon, Discovery of gliotoxin as a new small molecule targeting thioredoxin redox system, Biochem. Biophys. Res. Commun. 359 (2007) 523–528, https://doi.org/10.1016/J.BBRC.2007.05.139.
[35] M. Fardi, M. Alivand, B. Baradaran, M. Farshdousti Hagh, S. Solali, The crucial role of ZEB2: From development to epithelial-to-mesenchymal transition and cancer complexity, J. Cell. Physiol. 234 (2019) 14783–14799, https://doi.org/10.1002/JCP.28277.
[36] A. Sathyanarayanan, K.S. Chandrasekaran, D. Karunagaran, microRNA-145 modulates epithelial-mesenchymal transition and suppresses proliferation, migration and invasion by targeting SIP1 in human cervical cancer cells, Cell. Oncol. (Dordr.). 40 (2017) 119–131, https://doi.org/10.1007/S13402-016-0307-3.
[37] M.C. Sobotta, W. Liou, S. Stöcker, D. Talwar, M. Oehler, T. Ruppert, A.N.D. Scharf, T.P. Dick, Peroxiredoxin-2 and STAT3 form a redox relay for H2O2 signaling, Nat. Chem. Biol. 11 (2015) 64–70, https://doi.org/10.1038/NCHEMBIO.1695.
[38] A.T. Shaw, S.-H.I. Ou, Y.-J. Bang, D.R. Camidge, B.J. Solomon, R. Salgia, G.J. Riely, M. Varella-Garcia, G.I. Shapiro, D.B. Costa, R.C. Doebele, L.P. Le, Z. Zheng, W. Tan, P. Stephenson, S.M. Shreeve, L.M. Tye, J.G. Christensen, K.D. Wilner, J.W. Clark, A. J. Iafrate, Crizotinib in ROS1-rearranged non-small-cell lung cancer, N. Engl. J. Med. 371 (2014) 1963–1971, https://doi.org/10.1056/NEJMOA1406766.
[39] A.M. Fortier, E. Asselin, M. Cadrin, Keratin 8 and 18 loss in epithelial cancer cells increases collective cell migration and cisplatin sensitivity through Claudin1 up-regulation, J. Biol. Chem. 288 (2013) 11555, https://doi.org/10.1074/JBC.M112.428920.
[40] D. Sun, M. Zhou, C.M. Kowolik, V. Trisal, Q. Huang, K.H. Kernstine, F. Lian, B. Shen, Differential expression patterns of capping protein, protein phosphatase 1 and casein kinase 1 may serve as diagnostic markers for malignant melanoma, Melanoma Res 21 (2011) 335, https://doi.org/10.1097/CMR.0B013E328346B715.
[41] M.A. El Sharouni, R.V. Rawson, V. Sigurdsson, A.J. Witkamp, C.H. van Gils, R. A. Scolyer, J.F. Thompson, P.J. van Diest, S.N. Lo, The progressive relationship between increasing Breslow thickness and decreasing survival is lost in patients with ultrathick melanomas (≥15 mm in thickness), J. Am. Acad. Dermatol. 87 (2022) 298–305, https://doi.org/10.1016/J.JAAD.2022.01.040.
[42] R.A. Scolyer, R.V. Rawson, J.E. Gershenwald, P.M. Ferguson, V.G. Prieto, Melanoma pathology reporting and staging, Mod. Pathol. 33 (2020) 15–24, https://doi.org/10.1038/S41379-019-0402-X.
[43] D. Kubota, K. Mukaihara, A. Yoshida, H. Tsuda, A. Kawai, T. Kondo, Proteomics study of open biopsy samples identifies peroxiredoxin 2 as a predictive biomarker of response to induction chemotherapy in osteosarcoma, J. Proteom. 91 (2013) 393–404, https://doi.org/10.1016/j.jprot.2013.07.022.